Universal features in lifetime distribution of clusters in hydrogen bonding liquids

Ivo Juki¢, Martina Požar, Bernarda Lovrinčević, Aurélien Perera

Universal features in lifetime distribution of clusters in hydrogen bonding liquids

Ivo Jukić[†,‡] , Bernarda Lovrinčević[‡,*], Martina Požar[‡], and Aurélien Perera[†,†]

September 27, 2021

[†]Laboratoire de Physique Théorique de la Matière Condensée (UMR CNRS 7600), Sorbonne Université, 4 Place Jussieu, F75252, Paris cedex 05, France.

[‡]Department of Physics, Faculty of Sciences, University of Split, Ruđera Boškovića 37, 21000, Split, Croatia.

Abstract

Hydrogen bonding liquids, typically water and alcohols, are known to form labile structures (network, chains, etc...), hence the lifetime of such structures is an important microscopic parameter, which can be calculated in computer simulations. Since these cluster entities are mostly statistical in nature, one would expect that, in the short time regime, their lifetime distribution would be a broad Gaussian-like function of time, with a single maximum representing their mean lifetime, and weakly dependent on criteria such as the bonding distance and angle, much similarly to non-hydrogen bonding simple liquids, while the long time part is known to have some power law dependence. Unexpectedly, all the hydrogen bonding liquids studied herein, namely water and alcohols, display highly hierarchic three types of specific lifetimes, in the sub-picosecond range 0-0.5ps The dominant lifetime very strongly depends on the bonding distance criterion and is related to hydrogen bonded pairs. This mode is absent in non-H-bonding simple liquids. The secondary and tertiary mean lifetimes are related to clusters, and are nearly independent of the bonding criterion. Of these two lifetimes, only the first one can be related to that of simple liquids, which poses the question of the nature of the third lifetime. The study of alcohols reveals that this 3rd lifetime is related to the topology of H-bonded clusters, and that its distribution may be also affected by the alkyl tail surrounding ?bath?. This study shows that hydrogen bonding liquids have a universal hierarchy of hydrogen bonding lifetimes with a timescale regularity across very different types, and which depend on the topology of the cluster structures

[*]bernarda@pmfst.hr

[†]corresponding author (aup@lptmc.jussieu.fr)

1 Introduction

Labile structures in associated liquids and mixtures pose the problem of the role of kinetics of said structures, and its influence on the thermophysical and dynamical properties of these systems [1, 2]. Such structures play an important role in soft matter, as for example with micelles and lamellae [3, 4, 5], and more particularly in biology, wherein the labile character of various functional molecular entities, such as enzymes for example, wears a fundamental operational nature [6, 7, 8]. One might even postulate that biological systems have been built by the increasing role played by such labile structures in the early evolution of primitive biochemical systems [9, 10]. Based on these premises, it is important to better understand the interplay between labile nature of molecular assemblies and the role of kinetics in their dynamics [1, 6, 7, 8].

A first step in that direction would be to analyze the lifetime distribution of the hydrogen bonding process which is at the root of molecular association [11, 12]. Since H-bonding is essentially a quantum mechanical process, it is affected by various intramolecular motions, and in turn it affects intermolecular motions. It is not clear if the various experimental techniques, which allow to probe the frequencies associated with these motions, can unambiguously answer the question posed above [13, 14, 15, 16]. Since this is a many body quantum mechanical phenomenon, it is not even clear if classical approximate theories can provide an alternative approach to this question. On the other hand, computer simulation provide a direct access to the statistics of molecular motions, and are able to answer this question. One could even answer this question at the level of classical physics, where the hydrogen bond is modeled by the Coulomb pairing of opposite charges [17, 18], and whose pertinence has been amply proven by more than fifty years of computer simulations and force field development.

In fact, the question posed above has been already partly answered by Luzar and Chandler in their 1996 Nature paper [19]. In this paper, the authors focus essentially in the long time kinetics of H-bonding in water, beyond the initial 0.5 ps which they mention as the transient regime. This choice is amenable to a theoretical approach of the H-bonding kinetics, which is shown to be non-exponential, and further supported by classical computer simulations, but it does not explain the origin of the transient behaviour observed at short times. The present work aims at revealing surprising repeatability of this transient part across several H-bonding liquids. It is initially motivated by the fact that H-bonding liquids other than water, such as alcohols and amines, are known to form short chain-like clusters, both from scattering experiments [20, 21, 22, 23, 24, 25, 26, 27, 28, 29, 30, 31, 11, 32], spectroscopy investigations [33, 34, 35, 36, 37] and computer simulations [38, 39, 40, 41, 42, 43, 44]. Exploring this transient regime, essentially in the sub picosecond region, we have uncovered a universal dynamical behaviour common to all H-bonding liquids, which is unexpected in this time domain, where the differences in the molecular interactions play an important role. Indeed, such universality would be more expected in the long time kinetics regime, where common features of the association process are likely to settle [2, 45].

In order to better appreciate the results presented herein, it is useful to picture the H-bonding process as essentially a random process at short times and distances, governed by the random molecular encounters. Intuitively, one would expect a broad distribution of H-bonding life times, as function of both time and H-bonding distance, centered around some mean representative lifetime, which could be subsequently searched in the various experimental techniques investigating the relaxation processes. What we uncover here, is that while the distribution of H-bonding distances are indeed as hypothesized, the lifetime distributions exhibit several specific times, which vary from 1 at very short distances to 3 at larger ones, where the distances are picked around the main peak of the oxygen-oxygen distribution function, typically in the range $2.5\mathring{A}$ to $3.5\mathring{A}$, this latter value being often used in the literature [46, 47, 48, 49], as in the Luzar paper mentioned above [19]. These specific times, and related distribution, appear as common to all three associated liquids we have investigated herein, namely water, alcohols and amine, and across different force field representation. In contrast, the long time kinetics show specificities related to each type of liquid. Although we have used classical force field, this universality strongly suggests that these times should be a real feature of the associated liquids. We suggest that these specific times correspond to three types of molecular associations: dimer, linear chain-like clusters and other types of clusters. This finding suggests that self-assembled labile structures have typical lifetimes related to their differences in microscopic topology. In that, it helps understand how such structures, when complexified by appropriate molecular entities, could acquire an important role in the pre-biotic phenomena. More importantly, it shifts the interest to such structures, from the usual long time kinetics approach, where kinetic constants play an important role, to short times and distance, in the range of which new self assembled objects appear, and could possibly play the role of new molecular species in a very restricted spatio-temporal region.

2 Theoretical, models and simulation details

We would like to first stress that the present manuscript deals with the H-bond lifetime distribution itself, and not the time auto-correlation of it, which has been the subject of previous works by other authors [19, 50, 51, 52, 53]. It is therefore important to clarify the differences in the theoretical backgrounds. The hydrogen bond is a real property of many associated liquids in many contexts. However, for calculation purposes, it is necessary do define the two following parameters, the bonding distance r_c between the two donor/acceptor atoms, and the corresponding bonding angle θ_c. In computer simulations, two molecules i and j are considered as H-bonded, when the distance r_{ij} between the corresponding donor/acceptor atoms A_i and B_j obeys $r_{ij} \leq r_c$, and the angle $\theta_{ij} = \widehat{A_iHB_j}$ obeys $|\theta_{ij}| < \theta_c$. The A_i and B_j atoms are typically oxygen atoms, such as in water, but they can also refer to nitrogen atoms, such as for 1-propylamine considered in this work. Below, we will refer as $\mathcal{C}$ the ensemble of atoms which verify both criteria. For each pair of molecules in this time inter-

val, there are 2 characteristic times: that t_{ij} when they first bond and τ_{ij} when they break apart for the first time. For this pair, we define a time dependent random variable $H_{ij}(t)$, such that

$$H_{ij}(t) = H(t - t_{ij})H(\tau_{ij} - t) \tag{1}$$

where $H(t)$ is the Heaviside function, and $H_{ij}(t) = 1$ for $t_{ij} < t < \tau_{ij}$ and zero elsewhere.

We believe that this is the first proper definition of the function introduced in the previous literature [19, 50, 51, 52, 53] under the denomination $h(t)$. From this random variable one can measure several statistical averages and correlation, and in particular the auto-correlation function $c(t) =< h(0)h(t) >$ which has been studied in the past.

In the present work, we focus on the lifetime distribution itself, and the appropriate random variable is $h_{ij}(t)$ can defined from $H_{ij}(t)$. We first take the derivative $dH_{ij}(t)/dt = \delta(t - t_{ij}) - \delta(t - \tau_{ij})$, and remove the origin part. Then we define $h_{ij}(t)$ as gauge variable (because of the derivative/integration operations) related to $H_{ij}(t)$ through

$$h_{ij}(t) = \int dt \delta(t - \tau_{ij}) \tag{2}$$

which is 1 when the H-bond breaks at time τ_{ij} and zero elsewhere.

This variable is therefore adapted to built the lifetime histogram, and the associated lifetime distribution defined as

$$L(t) = \frac{1}{T_0 L_0} \sum_{ij \in \mathcal{C}} h_{ij}(t) \tag{3}$$

where the normalisation factor L_0 is defined as

$$L_0 = \frac{1}{T_0} \int_0^{T_0} dt \left[\sum_{ij \in \mathcal{C}} h_{ij}(t) \right] \tag{4}$$

It is easily verified that $L(t)$ is a probability distribution which verifies

$$\int_0^{T_0} dt L(t) = 1 \tag{5}$$

Eqs.(3,4) provide a direct computational indication as how to evaluate $L(t)$ in a given computer simulation. An average over all possible time origin is implict. The auxiliary Gromacs program *gmx hbon*d module with the *-life* option, allows to compute $L(t)$. We have also checked through our own code that it was consistent with the definitions given above. It should be noted that one can end the H-bonding as soon as two bonded atoms part away according to the chosen criterion. This is the strict definition, which has been adopted in this work, but also in Gromacs. However, in reality, a broken bond could be reformed quickly, and perhaps some margin should be allowed for rebinding, which could

be added to the ensemble of criterion in $\mathcal{C}$. This could be conveniently introduced by replacing the Dirac delta in Eq.(2) by a Gaussian function, which we will consider in another context.

This study focuses on the typical hydrogen bonding liquids, which are water and alcohols, which are both based on the OH group. Mono-ols such as methanol, ethanol and propanol have been studied. The SPC/E [54] and TIP4P_2005 [55] models were used to simulate water. Alcohols were modeled with the OPLS-UA [56] and TRaPPE-UA [57] forcefields.

The program package Gromacs, version 2018.1 [58, 59] was used for all molecular dynamics simulations. The simulation protocol has been the same for all neat systems. The initial configurations of N molecules were generated by random molecular positioning with the program Packmol [60], which were then energy minimized. The values for N considered here are typically N=1000 or N=2048. The systems were then equilibrated in the isobaric constant NpT ensemble for at least 5 ns, followed by a production run of at least 5 ns. Finally, an additional production run of 300 ps was performed to gather sufficient data for the analysis of dynamic quantities (every configuration was sampled).

The integration algorithm of choice was the leap-frog [61] and the time step was 2 fs. The electrostatics were handled with the PME method [62] and the constraints with the LINCS algorithm [63]. The short-range interactions were calculated within the 1.5 nm cut-off radius. Each neat liquid was simulated at ambient conditions. Temperature was maintained at T = 300 K using the Nose–Hoover [64, 65] thermostat, while pressure was kept at p = 1 bar with the Parrinello–Rahman barostat [66, 67]. The temperature algorithms had a time constant of 0.2 ps, while the pressure algorithm was set at 2 ps.

The lifetime calculation is part of the post simulation analysis Gromacs package (*gmx H-bond* module) . It follows the usual process of monitoring the lifetime of pairs of H-bonded O atoms across different water molecules. The O-O H-bonding distance r_c and the O-H-O angle are input parameters. In this study, while we vary the bonding distance, the angle is maintained to the accepted value of $180°\pm30$. However, the angular dependence is briefly discussed in section 3.5, and shown to be very similar to the distance dependence.

3 Results

Usually, H-bonding is discussed in terms of the spatial distribution, through pair correlation functions and their spatial representations, as proven by their overwhelming representation in the literature, as compared with their temporal one. Therefore, the finding of a corresponding temporal universality can be considered as an important feature, which should help better understand the role of labile structures.

3.1 Static structural properties of H-bonding

The universality in kinetics claimed in this work is supported by the static properties, in particular by the structural properties. Fig.1 shows the various oxygen-oxygen pair correlation functions $g_{OO}(r)$ obtained from computer simulations of the SPC/E water model, and first two OPLS alcohol models. The first peaks, shown in the main panel, demonstrate that the contact pairing is dominated by the oxygen atom size as well as the strong H-bonding pairing induced by the O-H-O Coulomb association. It is important to note that these first peaks are relatively robust across models, such that the distributions of bonding distances do not vary much across models. This is further enforced by the striking resemblance of distribution times across models, as shown below and in the SI material.

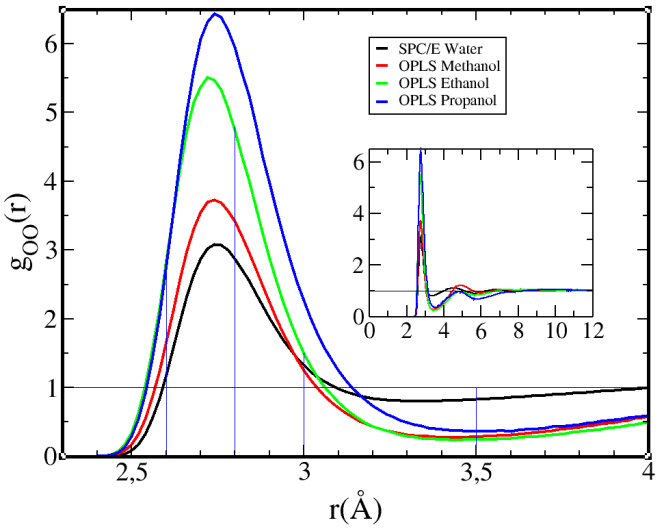

Figure 1: Oxygen-oxygen distribution functions $g_{OO}(r)$ for water and first alcohols. The vertical blue lines represent a sample of the H-bonding distances used in this work. The inset represent a wider range of these functions.

We turn to the H-bond donor-acceptor distance distributions, which is shown in Fig.2, for the same models as in Fig.1. $D_{HB}(r)$ is defined as the histogram of the number of bonded pairs for a given distance r, and calculated here for systems of N=2048 molecules. We immediately note the expected feature discussed in the Introduction, namely that the distribution is indeed a broad one, centered around a distance which corresponds to the central peak in Fig.1, around $2.7\mathring{A}$. It confirms that the underlying bonding is essentially randomly distributed. This finding is somewhat in contrast with what snapshots of the cluster analysis reveal, where such clusters in water appear in various patterns, while for alcohols it has been proven that chains and loops are predominant.

The curves in Fig.2 tend to indicate that donor-acceptor distribution is es-

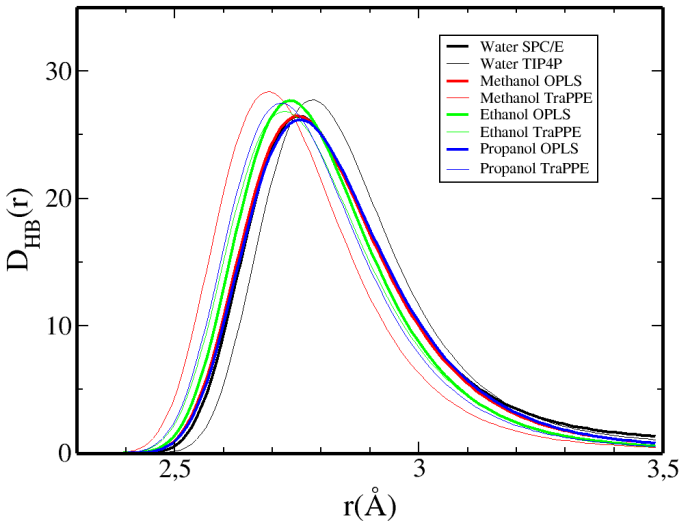

Figure 2: H-bond spatial distribution function $D_{HB}(r)$ for the different models studied herein.

sentially dominated by the dimers. Differences in clustering are found in the larger distance in $g_{OO}(r)$, which is shown in Fig.1. Indeed, it is seen in the inset of Fig.1 that the $g_{OO}(r)$ of the alcohols appears more depleted in the distance range $4 - 6\mathring{A}$, which indicates that chain clusters are predominant in alcohols [40, 41, 32]. A direct consequence of this difference in clustering is the fact that the scattering intensities of alcohols differ markedly from that of water, since they exhibit a pre-peak. [22, 23, 24, 25, 28, 32]. Perhaps the next most striking feature in Fig.2 is the near exact superposition of all the curves, indicating that the H-bonding between oxygen atoms is near invariant across molecular species. Small variations are attributable to parameter differences in the underlying classical force field, such as the partial charges and atom Lennard-Jones parameters. The equivalent of Fig.2, but the angular distribution is shown in the SI document in Fig.SI-1, and shows very similar general pattern, as illustrated for water and ethanol.

In many previous works different authors [68, 69, 70], including us [40, 41, 71, 44, 32], have studied the H-bonded cluster distributions. Some of such results are shown in the SI document under Fig.SI-2. Some typical clusters are shown for water and alcohols, highlighting the chain-like patterns. These results indicate that different observables, such as that in Fig.1 and Fig.SI-1, and that in Fig.SI-2, show very different trends.

The analysis above clearly indicates that the clustering differences between water and alcohols cannot be clearly differentiated through the spatial H-bond distribution analysis, which in a way is disappointing. But, we show now that this is not the case for the temporal distributions.

3.2 H-bond life times

We would like to stress that it is the lifetime of pair of associated atoms which is measured, and not that of clusters. One expects that the pair lifetime would influence the cluster lifetime by some broadening or narrowing of the distribution. But what we observe below is unexpected.

3.2.1 Water

Fig.3 shows the H-bond lifetimes distributions $L_{HB}(t)$ for the SPC/E water model, in log-scale, for different distances encoded in the color codes of the different curves, and ranging from $r_c = 2.5\mathring{A}$ to $r_c = 3.5\mathring{A}$, which cover the distances from under the first peak in Fig.1 until the first minimum. In terms of the corresponding oxygen-oxygen potential of mean force, such as -ln($g_{OO}(r)$), these correspond to the first neighbour ranges, as shown in Fig.1, for example. Fig.3 shows two remarkable features. First, for small distance $r_c < 3.0\mathring{A}$, one sees a series of peaks, centered around a single maximum which represents the mean bonding lifetime, and these peaks are seen to shift to larger times as r_c is increased, as well as decreasing in magnitude. The shift to larger times can be explained as the bonding distance criteria is brought closer to the first maximum of $g(r)$ and beyond, one increases the probability of pair association stability, hence the mean lifetime.

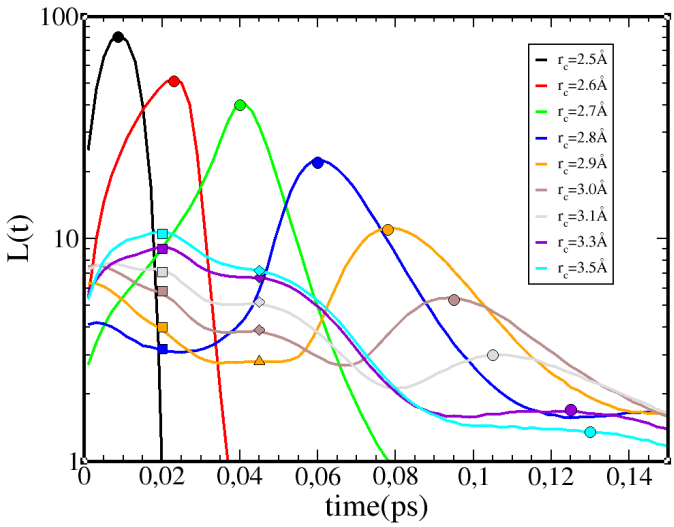

Figure 3: H-bond lifetime distribution $L(t)$ for SPC/E water, with different H-bonding distances r_c. The symbols on each curve signal the corresponding peak position (see text): dot for first peak, square for second and triangle for third.

However, as the contact distance is increased, we witness the appearance of 2 secondary peaks, which grow at shorter times than the corresponding first

peak lifetime. For example, for the mean H-bonding distance of $r_c = 2.7\mathring{A}$ (green curve), the main peak is at 40 fs, while a broad shoulder at 15 fs witness the growth of the two secondary lifetimes. For the largest H-bonding distance of $r_c = 3.5\mathring{A}$ (in cyan), the secondary peaks are respectively at 20fs and 45fs, and their amplitude is far superior to that of the first peak/shoulder at 130fs, since they are respectively of 10 and 7, almost one order of magnitude larger that the for the first peak. In addition, we see that these two secondary peaks are nearly always at the same respective times of 20fs and 45fs. Anticipating the corresponding analysis for the alcohols, we infer that these 2 secondary peaks must correspond to lifetimes of bonded pairs within larger clusters, hence are signatures of such clusters. The overall picture which emerges from these findings is that, tightly H-bound molecules (small r_c) have high probability but short lifetimes, but less tightly H-bound molecules (larger r_c) are less probable, but live longer since they belong to a cluster. But a new problem appears: if the secondary peaks corresponds to H-bonding within a cluster, why two such peaks? Following the same inferring approach, we deduce that two types of clusters are present. From the analysis of the cluster shapes in water, and also in alcohols, we infer that these peaks must correspond respectively to linear and non-linear (globular, or branched) clusters.

Figs.SI-1 and SI-2 of the SI material show that the shape of these lifetimes is very similar across water models. It must therefore be a genuine physical property of real water.

Finally, we note that the conclusions inferred from the analysis above are in contrast to a generic intuitive idea: that clusters could be made of highly and tightly H-bound molecules. The picture which emerges from the present analysis is that larger clusters are less probable than dimers, but they are also live longer. At the opposite range, dimer clusters are highly likely, but they also break faster than larger clusters. Somewhere in between these two extremes, one must have clusters which witness the existence of labile entities, and the 3 peaks of the present finding correspond to typical such clusters.

We now in position to confront our findings with respect to that of Luzar and Chandler [19]. Fig.4 shows the long time behaviour of $L(t)$. It is readily seen that, as the H-bonding distance is increased, the fast exponential decay corresponding to smaller H-bonding distances converges towards a slow, and possibly non-exponential behaviour, as witnessed by the merging of the 3 curves corresponding to the range $r_c = 3.1 - 3.5\mathring{A}$. Luzar and Chandler have selected $r_c = 3.5\mathring{A}$ in their entire analysis, and this criterion seems to have been retained in all subsequent literature [47, 48, 49]. In view of the present analysis, this approach would correspond to a global, almost macroscopical view of the kinetics of association in H-bonded liquids. While this may seem reasonable to make contact with macroscopic physics, we show here that the microscopic physics does not lead to a picture dominated by random distributions, but on the contrary to a selective trinitary view of clustering.

What about other H-bonded liquids? These are usually not studied under the same perspective as water. For example, H-bonding in water is often discussed in terms of flickering clusters [72] or network [73]. These specificities

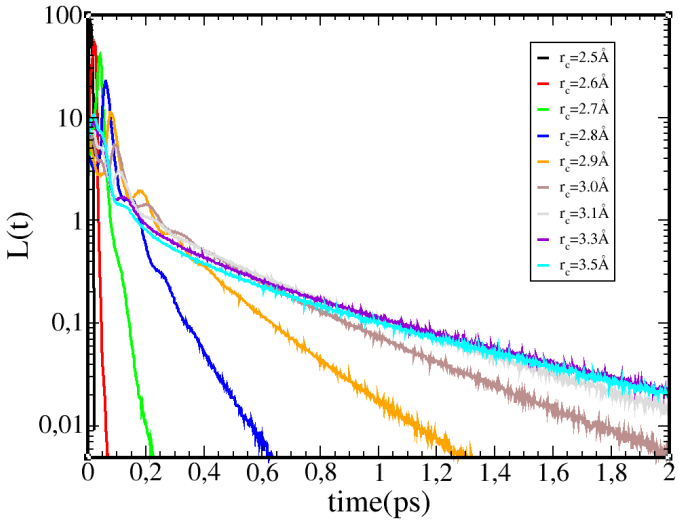

Figure 4: Long time behaviour of the H-bond lifetime distribution $L(t)$ for the SPC/E model.

do not apply to other H-bonding liquids throughout the literature. Is there a common clustering specificity to all H-bonding liquids?

3.2.2 Alcohols

Fig.5 shows the H-bond lifetimes distributions $L(t)$ for the OPLS methanol model. The comparative analysis for other models is shown in the SI document. A comparison of Fig.5 with water in Fig.3 shows immediately that the same global features are present, namely a high first peak which decreases to larger lifetimes for larger r_c distances, while intermediate 2 lifetime peaks emerge at distances around the attractive minimum of the mean force potential.

The principal differences are seen in the values of the maximum amplitudes and positions, which are model dependent to a large extent as one should expect for underlying differences in interactions, but also in the secondary peaks. These latter peaks appear as more marked for methanol than for water, and this is more particularly true for the second peak, which is a true peak for the alcohol, while it was more of a shoulder in the case of water. Another similarity with water is the relative insensitivity of the positions of the second and third peaks to the H-bonding r_c distance. The fact that the secondary peaks are more marked is in line with the known fact that alcohols form linearly shaped clusters [22, 23, 24, 28] of different topology: chains, loops, lassos [74, 75, 25, 30, 27]. These shapes are not found in water, at least in computer simulation of popular water models. Therefore, the similarity of the peak cannot refer to topological specificity, but to characteristic H-bonding patterns. The cluster analysis of water models shows that water clusters are either globular like or chain like. A

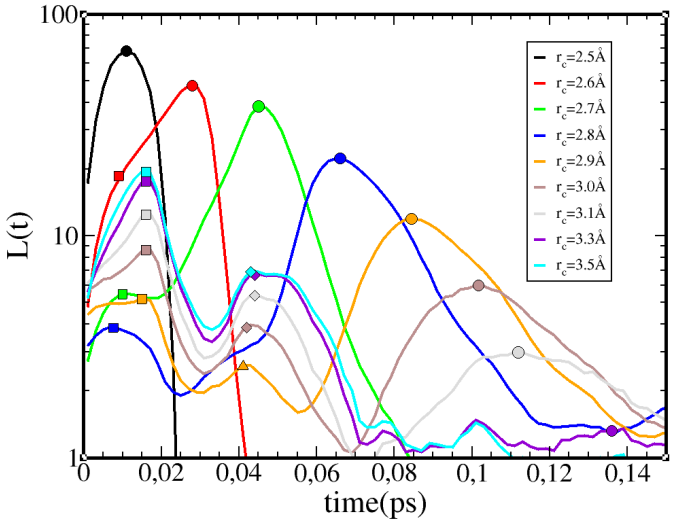

Figure 5: H-bond lifetime distribution for OPLS methanol, with different H-bonding distance r_c. Symbols and line colors are same as in Fig.3

similar analysis for the alcohols indicates that linear and branched clusters are mostly present.

Fig.6a and Fig.6b show similar distributions for OPLS ethanol and propanol, as well as Fig.6 of the SI for 1-octanol. Again, the similarity with both methanol and water is striking and enforces the idea that the clustering features of the hydroxyl group are pretty much the same across different H-bonding liquids bearing this group, such as water and mono-ols.

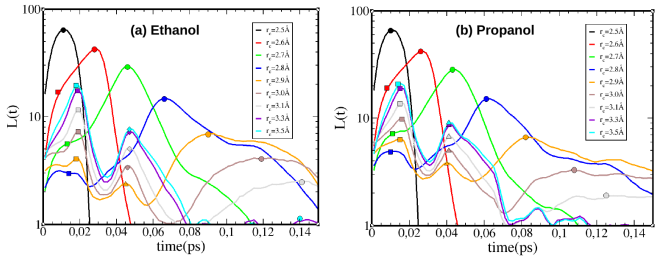

Figure 6: H-bond lifetime distribution for OPLS ethanol (a) and propanol (b), with different H-bonding distance r_c. Symbols and line colors are same as in Fig.3

The case of 1-propylamine is illustrated in Fig.7 of the SI, and again shows very similar features for L(t), although this is a very different H-bonding liquid

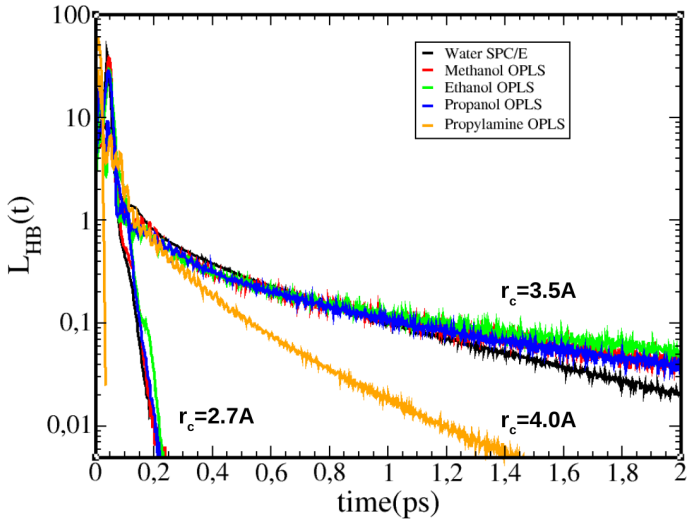

Figure 7: Long time behaviour of the H-bond lifetime distribution for all the models studied herein

with the amine group NH2, and an acceptor nitrogen atom which is larger than the oxygen atom of water and hydroxyl groups of alcohols. Hence, the distances associated to each curves are different than those in Figs(3,4). This particular liquid confirms that the short time universality for L(t) uncovered herein is a real feature of H-bonding liquids in general.

Similarly to Fig.4 for water, we compare in Fig.7 the long time decay of L(t) for several H-bonding liquids, and this for two different values of r_c. Interestingly, we find that for a given r_c, all curves tend to lie quite close to one another, and that there is also a species dependence. This is illustrated for $r_c = 3\mathring{A}$ for water and alcohols. We also note that, since 1-propylamine is a nitrogen based H-bonding liquid, its long time behaviour cannot be compared with that of oxygen atom based ones. It is interesting to compare the long time analysis of $L(t)$ with the approach of Luzar-Chandler which is based on the analysis of $c(t)$ and the related H-bond kinetics. While the long time behaviour points to differences in H-bonding liquids, the short time transient part, which we study here demonstrates, that the underlying transient dynamics are based on universal elementary cluster structures. This is perhaps the main message of the present findings.

3.3 A test with the "weak-water" model

In order to test the present conclusions, and in particular the inference methodology, we have studied previously introduced models of "weak-water" [76]. This model is based on the SPC/E water for water, where the partial charges on the oxygen and hydrogen atoms are scaled by a parameter λ ($0 < \lambda < 1$), allowing

to tune the hydrogen bonding from the original model (with $\lambda = 1$) to a simple Lennard-Jonesium (with $\lambda = 0$). It was found that from $\lambda \leq 0.6$ the influence of partial charges and hydrogen bonding were not relevant and the model was structurally similar to a simple Lennard-Jones liquid. This model appears here as a useful way to measure the cluster hypothesis for the complex time dependence of $L(t)$. As λ is made smaller, the hydrogen bonding abilities decrease, and it is possible to test directly the influence of hydrogen bonding clusters on the shape of $L(t)$.

In the order to preserve the liquid state for small λ values and under ambient conditions, it was found necessary to increase the Lennard-Jones energy parameter $\epsilon = \epsilon(\lambda)$ according to the decrease of λ. In the present test, we have bypassed this procedure by doing the test simulations in the NVT Canonical ensemble, hence keeping the volume fixed at that of the real liquid water.

Since the structure of the weak-water liquid is strongly be affected by the decrease of the partial charges, the H-bonding distances must be adjusted appropriately. Fig.8a shows the various $g_{OO}(r)$ for different λ values we have used here, namely $\lambda = 0.8$, 0.5 and 0.2. The selected bonding distances depend on the position of the maximum, and differ quite a bit from that of the initial SPC/E water, ranging now from $2.7\mathring{A}$ to $4.5\mathring{A}$. It is important to note that, while we vary the bonding distance criteria, we keep the angular criterion the same as that for pure water, which is that the angle O-H-O is 180 ± 30. This means that, even though weaker water model may have different bonding angles, we will still select only a sub class of those obeying tetrahedral bonding directions. This is justified by the fact that these models do not have as strong H-bonding tendencies as SPC/E water, hence the angular bias is less significant than the distance of bonding. But we will need to take into this bias in order to interpret the data.

Fig.8b shows the H-bond lifetimes for $\lambda = 0.2$, which is very close to a Lennard-Jones system. For very small bonding distances $r_c \leq 3.0\mathring{A}$, we note that the $L(t)$ do not exhibit a clear maximum, and sometimes even show a plateau-like behaviour, such as for $R = 3.0\mathring{A}$(blue curve). This is a direct consequence of the angular bias described above. However, from bonding distance $r_c \geq 3.1\mathring{A}$, we observe a clear maximum, and this maximum is nearly the same for all subsequent r_c values. This is what we would expect in a quasi-LJ system, where pairing is nearly isotropic. We also note that this lifetime distribution is not necessarily about isolated pairs, and could involve those in larger clusters. We note the presence of intriguing small shoulder-like features at large times, such as for the green, blue and yellow curves, but these features cannot be interpreted from Fig.8b alone, but will become clearer from the analysis of the next cases.

Fig.8c shows the H-bond lifetimes for $\lambda = 0.5$, which has the same pair distribution as the $\lambda = 0.2$ case, as seen in Fig.8a. We note that most of the features observed previously equally appear here - supporting the structural analogy, but the previously noted intriguing shoulder structures has now grown into peak structures and are very apparent. However, it still remain difficult to interpret them by simple inference.

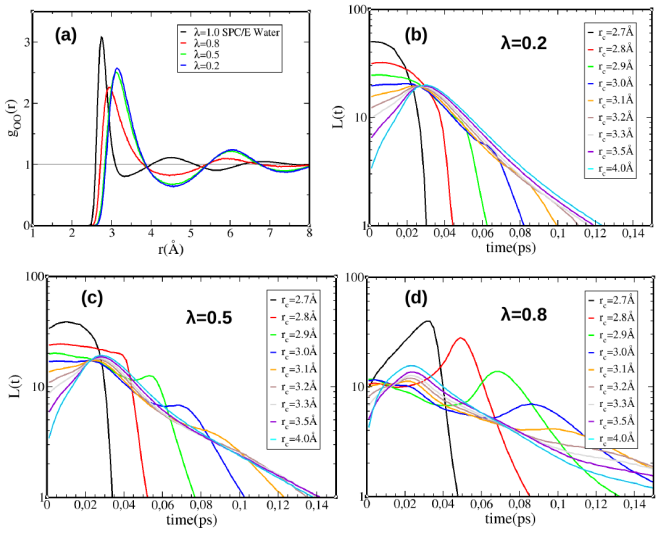

Figure 8: Weak water models data. (a) Comparison of the RDF of various models; (b) H-bond lifetimes for $\lambda = 0.2$; (c); (b) H-bond lifetimes for $\lambda = 0.5$; (d) H-bond lifetimes for $\lambda = 0.8$.

Fig.8d is for the case $\lambda = 0.8$, which is the closest to SPC/E water, and should be compared with Fig.3. The previous intriguing peaks have now grown to invade the entire figure, and, by comparison with Fig.3, represent the dominant contribution to the H-bond lifetimes for each R r_c value, as we have interpreted them when discussing Fig.3. But now, we can finally understand the smaller features in Fig.8c, namely the origin of the secondary peaks, precisely because these were the dominant features in the previous Figs.8b-c. Indeed, we have interpreted them as peaks related to bonded pairs within clusters. This is precisely the conclusion we have reached when discussing Figs.3-6, but by inference. To summarize, the study of the weak-water models allow us to confirm that the secondary peak features are indeed related to clusters.

3.4 Influence of the alkyl tails

Although the present study reveals similarities in the H-bonding life times, one would expect that the presence of non-bonding alkyl tails would affect the lifetime. This is illustrated in Fig.9 for all the liquids studied in this work, water, methanol to 1-octanol and 1-propylamine. Since the alkyl tail influence is best seen at largest distance cutoff we have considered $r_c = 3.5\mathring{A}$ for all systems except for propylamine, for which we have used appropriately $r_c = 4.0\mathring{A}$.

For clarity, each curve has been shifted by log(10) from the previous one. The bottom black curve is for water, and serves only as a reference, since water has no alkyl tail, and consequently does not show anything particular other

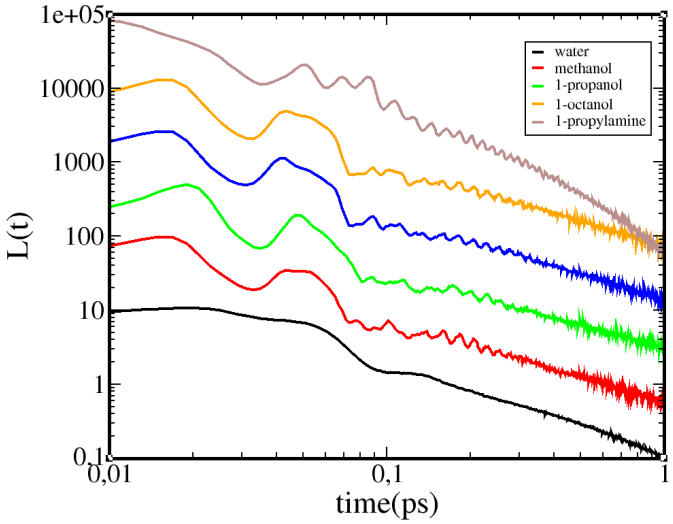

Figure 9: Influence of alkyl tails on lifetime distribution for methanol (red), ethanol (green), propanol(blue), octanol (gold) and propylamine (purple). The black curve is for water and serves as a reference. The gray lines serve to delimitate the 2nd and 3rd peaks regions mentioned in the text.

than the features discussed above. However, all the alcohol curves show tiny oscillations past the 3rd peak. Higher alcohols such as 1-propanol and 1-octanol have even their 3rd peak weakly modulated. We attribute these oscillations in lifetime to the presence of the alkyl tail "bath", which surrounds the OH clusters, and affects the decay of their lifetime. This interesting feature further supports the interpretation that the 3rd peak is associated with the evolution of the cluster topology in time. This feature is naturally absent from water because there are no alkyl groups. However, the case of the propylamine (the upper most curve in purple) is very interesting. In previous studies [44], we have compared the clustering of neat 1-propanol to that of 1-propylamine, and shown that the clustering of the amine group was not so important, both in size and shape, as the chain patterns observed for 1-propanol. The alkyl chain, being the same between the 2 species, plays an indirect role in this incomplete clustering of the NH2 amine groups. What we observe in Fig.9 is that the role of the alkyl tail is so important that it "bites" into the 3rd peak which is about cluster topology, and makes even this peak look less characteristic compared to those of the alcohols. These oscillations also last longer than in the case of alcohols. This figure reveals the dynamical role played by the seemingly neutral alkyl tail background. The role of these tails was emphasized in a previous study [32] of the shape of the Xray pre-peak feature of alcohols. This role is confirmed through the present study.

3.5 Angle dependence of $L(t)$

We briefly discuss here the H-bond donor-acceptor θ angle dependence of the lifetime distribution, which are seen to be quite similar to the r_c dependent ones. This is illustrated in Fig.10 for the SPC/E water model and the OPLS ethanol model. Since the overall behaviour of the primary dimer peak is very similar, only the secondary and tertiary peaks are shown for fixed H-bonding distance of $r_c = 3.5\mathring{A}$ corresponding to the minimum of $g_{OO}(r)$.

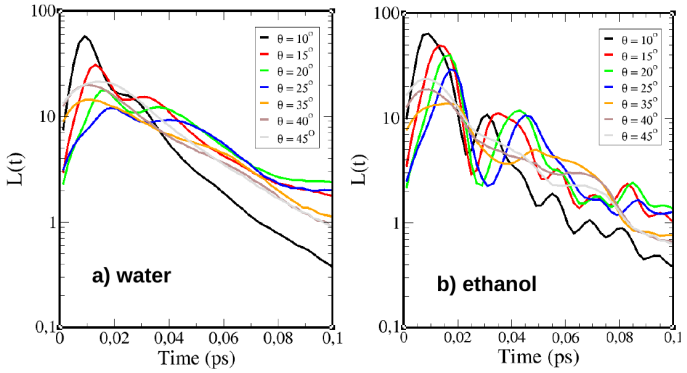

Figure 10: Angle dependence of H-bond lifetimes for SPC/E water (left panel) and OPLS ethanol (right panel). Only the secondary and tertiary peaks are shown for $r_c = 3.5\mathring{A}$

While the overall behaviour looks the same, we observe a notable difference in the dependence on θ of the two peaks, whereas in the case of the r_c dependence the peaks position were nearly invariant. We have attributed this invariance to that of the lifetimes of the clusters on r_c as soon as that value was large enough to account for cluster sizes. In the case of the angular dependence, we observe that clusters with larger allowed θ angles tend to live longer than those with more restricted ones. This appears to be a natural consequence of the fact that strong angle constraints lead to cluster breaking earlier. We conclude that the angle dependence is less a robust criteria than the distance dependence, in what concerns the universal behaviour. Finally, we note the alkyl tail dependence in the case of ethanol, with the presence of long time oscillations, very similar to those observed for the r_c dependence.

4 Discussion and Conclusion

While chemical matter, and more importantly bio-chemical matter, is known to be made of labile objects, in addition to well defined atoms and molecules. It raises the question whether such fleeting objects could play a role as important as the permanent ones. The pertinence of this question is enforced by the

recognition that liquid assemblies of atoms and molecules are subject to fluctuations which depend on the nature of the interactions, and in particular highly directional ones such as the H-bond interaction. Self assembly is the driving mechanism of many complex systems, such as in soft-matter and biological systems. The microscopic interaction at the root of self-assembly is the H-bonding process. This mechanism can be relatively well captured by classical force field simulation using Coulomb charge pairing.

The calculations reported herein show that, for a given H-bonding distance r_c, the H-bond lifetime is essentially dominated by one mean lifetime for distances r_c smaller than the first peak of $g(r)$, but that two secondary peaks appear for larger distances until the first minimum of $g(r)$, and that these become dominant as r_c is increased. We have attributed these peaks to linear and non-linear cluster geometries. In addition, the present study reveals a previously unexpected similarity in H-bonding lifetime distribution in the small distance and short time regime corresponding to distances under $3.5\mathring{A}$ and under 150 fs, and this independently of the nature of the H-bonding group. This interpretation is summarized in Fig.11 below, where we have shown sample L(t) curves for the SPC/E water (see Fig.3) for typical r_c distances picked along the first peak of the $g_{OO}(r)$ curve (see right panel), covering the contact, the peak height and 2 points at the minimum. The clusters shown above the right panel illustrate the first peak/dimer base (in red) within larger clusters (with additional water molecules shown in gray), helping to visualize why long lived dimers at larger r_c would give raise to shorter lived clusters.

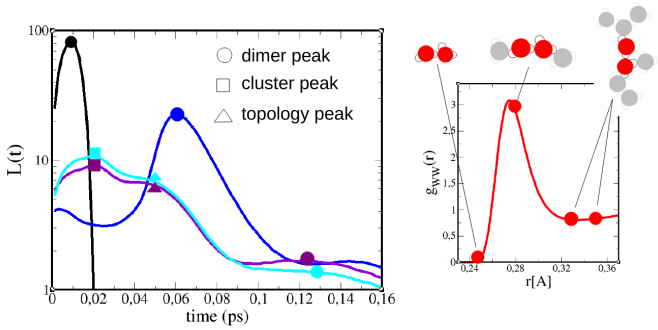

Figure 11: Illustration summarizing the correspondence between the hydrogen lifetime L(t) curves for different r_c values taken along the $g_{OO}(r)$ curve. The water molecules dimer based clusters illustrate the correspondence between first neighbours lifetimes and larger clusters lifetimes as r_c is varied.

We have provided convincing empirical arguments for the existence of three type of H-bond based clustering specificities in three different associated liquids, water, mono-ols and amines. These arguments suggest that there exist two distinct families of clusters, inside which the dimer lifetime plays a very different

role. The first family concerns linearly shaped clusters, whether these are line-like or circular. The second family, we have referred as non-linear clusters, which covers all other forms, such as globular -as those found in water, or branched, such as lasso-shaped found in mono-ols [77, 32].

The calculations concern primarily lifetime of pair of H-bonded particles. But such pairs often reside inside specific clusters, hence their lifetime is affected by the life of the entire cluster. Because of the cooperative motions of particles linked within a cluster, we expect that the these motions affect the lifetime statistics in particular ways, as to emerge the 3 peaks observed in the data reported herein.

Acknowledgments

This work has been supported in part by the Croatian Science Foundation under the project UIP-2017-05-1863 "Dynamics in micro-segregated systems".

References

[1] A. J. Goshe, I. M. Steele, C. Ceccarelli, A. L. Rheingold, and B. Bosnich. Supramolecular recognition: On the kinetic lability of thermodynamically stable host–guest association complexes. *Proceedings of the National Academy of Sciences*, 99(8):4823–4829, 2002.

[2] F. Paul, C. Wehmeyer, E. T. Abualrous, H. Wu, M. D. Crabtree, J. Schöneberg, J. Clarke, C. Freund, T. R. Weikl, and F. Noé. Protein-peptide association kinetics beyond the seconds timescale from atomistic simulations. *Nature Communications*, 8(1):1095, 2017.

[3] O. Glatter, G. Fritz, H. Lindner, J. Brunner-Popela, R. Mittelbach, R. Strey, and S. U. Egelhaaf. Nonionic micelles near the critical point:â micellar growth and attractive interaction. *Langmuir*, 16(23):8692–8701, 2000.

[4] S. De, V. K. Aswal, P. S. Goyal, and S. Bhattacharya. Novel gemini micelles from dimeric surfactants with oxyethylene spacer chain. small angle neutron scattering and fluorescence studies. *The Journal of Physical Chemistry B*, 102(32):6152–6160, 1998.

[5] J. Berghausen, J. Zipfel, P. Lindner, and W. Richtering. Influence of water-soluble polymers on the shear-induced structure formation in lyotropic lamellar phases. *The Journal of Physical Chemistry B*, 105(45):11081–11088, 2001.

[6] D. C. Augenstein, K. Thrasher, A. J. Sinskey, and D. I. C. Wang. Optimization in the recovery of a labile intracellular enzyme. *Biotechnology and Bioengineering*, 16(11):1433–1447, 1974.

[7] H. Spahn-Langguth and L. Z. Benet. Microsomal acyl glucuronidation: Enzyme-kinetic studies with labile glucuronides, 1993.

[8] Y. Kim, J. Park, and M.-J. Kim. Dynamic kinetic resolution of amines and amino acids by enzymeâmetal cocatalysis. *ChemCatChem*, 3(2):271–277, 2011.

[9] Jack T. Trevors and Roland Psenner. From self-assembly of life to present-day bacteria: a possible role for nanocells. *FEMS Microbiology Reviews*, 25(5):573–582, 12 2001.

[10] David Deamer, Sara Singaram, Sudha Rajamani, Vladimir Kompanichenko, and Stephen Guggenheim. Self-assembly processes in the prebiotic environment. *Philosophical transactions of the Royal Society of London. Series B, Biological sciences*, 361(1474):1809–1818, October 2006.

[11] L. Almásy, A.I. Kuklin, M. Požar, A. Baptista, and A. Perera. Microscopic origin of the scattering pre-peak in aqueous propylamine mixtures: X-ray and neutron experiments versus simulations. *Phys. Chem. Chem. Phys.*, 21:9317–9325, 2019.

[12] I. Jukić, M. Požar, and B. Lovrinčević. Comparative analysis of ethanol dynamics in aqueous and non-aqueous solutions. *Phys. Chem. Chem. Phys.*, 22:23856–23868, 2020.

[13] R. F. Lake and H.W. Thompson. Far infrared studies of hydrogen bonding in alcohols. *Proceedings of the Royal Society of London. Series A. Mathematical and Physical Sciences*, 291(1427):469–477, 1966.

[14] A. S. N. Murthy and C. N. R. Rao. Spectroscopic studies of the hydrogen bond. *Applied Spectroscopy Reviews*, 2(1):69–191, 1968.

[15] S.M. Craven and F.F. Bentley. Far infrared group frequencies. ii. primary amines. *Appl. Spectrosc.*, 26(4):449–453, May 1972.

[16] S.M. Craven and F.F. Bentley. Far-infrared group frequencies. i. aliphatic alcohols. *Appl. Spectrosc.*, 26(2):242–247, Mar 1972.

[17] W. L. Jorgensen. Quantum and statistical mechanical studies of liquids. 11. transferable intermolecular potential functions. application to liquid methanol including internal rotation. *Journal of the American Chemical Society*, 103(2):341–345, 1981.

[18] F. W. Starr, J. K. Nielsen, and H. E. Stanley. Hydrogen-bond dynamics for the extended simple point-charge model of water. *Phys. Rev. E*, 62:579–587, Jul 2000.

[19] A. Luzar and D. Chandler. Hydrogen-bond kinetics in liquid water. *Nature*, 379(6560):55–57, 1996.

[20] W.C. Pierce and D.P. MacMillan. X-ray studies on liquids: the inner peak for alcohols and acids. *Journal of the American Chemical Society*, 60:779–783, 1938.

[21] B.E. Warren. X-ray diffraction in long chain liquids. *Phys. Rev.*, 44:969–973, 1933.

[22] M. Magini, G. Paschina, and G. Piccaluga. On the structure of methyl alcohol at room temperature. *The Journal of Chemical Physics*, 77:2051–2056, 1982.

[23] A.H. Narten and A. Habenschuss. Hydrogen bonding in liquid methanol and ethanol determined by x-ray diffraction. *The Journal of Chemical Physics*, 80:3387–3391, 1984.

[24] K. S. Vahvaselkä, R. Serimaa, and M. Torkkeli. Determination of liquid structures of the primary alcohols methanol, ethanol, 1-propanol, 1-butanol and 1-octanol by x-ray scattering. *Journal of Applied Crystallography*, 28:189–195, 1995.

[25] A.K. Karmakar, P.S.R. Krishna, and R.N. Joarder. On the structure function of liquid alcohols at small wave numbers and signature of hydrogen-bonded clusters in the liquid state. *Physics Letters A*, 253:207–210, 1999.

[26] T. Yamaguchi, K. Hidaka, and A.K. Soper. The structure of liquid methanol revisited: a neutron diffraction experiment at â80 Â°c and +25 Â°c. *Molecular Physics*, 96:1159, 1999.

[27] C.J. Benmore and Y.L. Loh. The structure of liquid ethanol: A neutron diffraction and molecular dynamics study. *The Journal of Chemical Physics*, 112:5877–5883, 2000.

[28] M. Tomšič, A. Jamnik, G. Fritz-Popovski, O. Glatter, and L. Vlček. Structural properties of pure simple alcohols from ethanol, propanol, butanol, pentanol, to hexanol: Comparing monte carlo simulations with experimental saxs data. *The Journal of Physical Chemistry B*, 111:1738–1751, 2007.

[29] A. Sahoo, S. Sarkar, V. Bhagat, and R. N. Joarder. The probable molecular association in liquid d-1-propanol through neutron diffraction. *The Journal of Physical Chemistry A*, 113:5160–5162, 2009.

[30] A. Vrhovšek, O. Gereben, A. Jamnik, and L. Pusztai. Hydrogen bonding and molecular aggregates in liquid methanol, ethanol, and 1-propanol. *The Journal of Physical Chemistry B*, 115:13473–13488, 2011.

[31] J. Cerar, A. Lajovic, A. Jamnik, and M. Tomšič. Performance of various models in structural characterization of n-butanol: Molecular dynamics and x-ray scattering studies. *Journal of Molecular Liquids*, 229:346 – 357, 2017.

[32] M. Požar, J. Bolle, C. Sternemann, and A. Perera. On the x-ray scattering pre-peak of linear mono-ols and the related microstructure from computer simulations. *The Journal of Physical Chemistry B*, 124(38):8358–8371, 2020. PMID: 32856907.

[33] F. C. Hagemeister, C. J. Gruenloh, and T. S. Zwier. Density functional theory calculations of the structures, binding energies, and infrared spectra of methanol clusters. *The Journal of Physical Chemistry A*, 102(1):82–94, 1998.

[34] K. M. Murdoch, T. D. Ferris, J. C. Wright, and T. C. Farrar. Infrared spectroscopy of ethanol clusters in ethanolâhexane binary solutions. *The Journal of Chemical Physics*, 116(13):5717–5724, 2002.

[35] W. Wrzeszcz, M. Tomza, P.and Kwaśniewicz, S. Mazurek, R. Szostak, and M.A. Czarnecki. Microheterogeneity in binary mixtures of methanol with aliphatic alcohols: Atr-ir/nir spectroscopic, chemometrics and dft studies. *RSC Advances*, 6:37195, 2016.

[36] V. Pogorelov, Chernolevska. Y., Y. Vaskivskyi, L. G.M. Pettersson, I. Doroshenko, V. Sablinskas, V. Balevicius, J. Ceponkus, K. Kovaleva, A. Malevich, and G. Pitsevich. Structural transformations in bulk and matrix-isolated methanol from measured and computed infrared spectroscopy. *Journal of Molecular Liquids*, 216:53 – 58, 2016.

[37] M. P. Balanay, D. H. Kim, and H. Fan. Revisiting the formation of cyclic clusters in liquid ethanol. *The Journal of Chemical Physics*, 144(15):154302, 2016.

[38] T. Kosztolányi, I. Bakó, and G. Pálinkás. Hydrogen bonding in liquid methanol, methylamine, and methanethiol studied by molecular-dynamics simulations. *The Journal of Chemical Physics*, 118:4546–4555, 2003.

[39] R. Ludwig. The structure of liquid methanol. *ChemPhysChem*, 6:1369–1375, 2005.

[40] L. Zoranić, F. Sokolić, and A. Perera. Microstructure of neat alcohols: A molecular dynamics study. *The Journal of Chemical Physics*, 127:024502, 2007.

[41] A. Perera, F. Sokolić, and L. Zoranić. Microstructure of neat alcohols. *Physical Review E*, 75:060502(R), 2007.

[42] J. Lehtola, M. Hakala, and K. Hämäläinen. Structure of liquid linear alcohols. *The Journal of Physical Chemistry B*, 114:6426–6436, 2010.

[43] M. Požar, B. Lovrinčević, L. Zoranić, M. Mijaković, F. Sokolić, and A. Perera. A re-appraisal of the concept of ideal mixtures through a computer simulation study of the methanol-ethanol mixtures. *The Journal of Chemical Physics*, 145:064509, 2016.

[44] M. Požar and A. Perera. On the micro-heterogeneous structure of neat and aqueous propylamine mixtures: A computer simulation study. *Journal of Molecular Liquids*, 227:210, 2017.

[45] G Schreiber, G Haran, and H-X Zhou. Fundamental aspects of protein-protein association kinetics. *Chemical reviews*, 109(3):839–860, March 2009.

[46] M. Haughney, M. Ferrario, and I. R. McDonald. Molecular-dynamics simulation of liquid methanol. *The Journal of Physical Chemistry*, 91(19):4934–4940, 1987.

[47] E. Guardia, J. Martí, J.A. Padró, L. Saiz, and A.V. Komolkin. Dynamics in hydrogen bonded liquids: water and alcohols. *Journal of Molecular Liquids*, 96-97:3 – 17, 2002. Physical Chemistry of Liquids.

[48] Ioannis Skarmoutsos and Elvira Guardia. Local structural effects and related dynamics in supercritical ethanol. 2. hydrogen-bonding network and its effect on single reorientational dynamics. *The Journal of Physical Chemistry B*, 113(26):8898–8910, 2009. PMID: 19499904.

[49] J. Cerar, A. Jamnik, I. Pethes, L. Temleitner, L. Pusztai, and M. Tomšič. Structural, rheological and dynamic aspects of hydrogen-bonding molecular liquids: Aqueous solutions of hydrotropic tert-butyl alcohol. *Journal of Colloid and Interface Science*, 560:730 – 742, 2020.

[50] A. Luzar. Resolving the hydrogen bond dynamics conundrum. *The Journal of Chemical Physics*, 113(23):10663–10675, 2000.

[51] H. F. M. C. Martiniano and N. Galamba. Insights on hydrogen-bond lifetimes in liquid and supercooled water. *J. Phys. Chem. B*, 117(50):16188–16195, December 2013.

[52] V. P. Voloshin and Yu. I. Naberukhin. Hydrogen bond lifetime distributions in computer-simulated water. *Journal of Structural Chemistry*, 50(1):78–89, 2009.

[53] A. Geiger, P. Mausbach, J. Schnitker, R. Blumberg, and Stanley H. Structure and dynamics of the hydrogen bond network in water by computer simulations. *Journal de Physique Colloques C*, 45(C7):C7–13–C7–30, 1984.

[54] H. J. C. Berendsen, J. R. Grigera, and T. P. Straatsma. The missing term in effective pair potentials. *The Journal of Physical Chemistry*, 91(24):6269–6271, 1987.

[55] J. L. F. Abascal and C. Vega. A general purpose model for the condensed phases of water: Tip4p/2005. *The Journal of Chemical Physics*, 123(23):234505, 2005.

[56] W.L. Jorgensen. Optimized intermolecular potential functions for liquid alcohols. *The Journal of Physical Chemistry*, 90(7):1276, 1986.

[57] B. Chen, J.J. Potoff, and J.I. Siepmann. Monte carlo calculations for alcohols and their mixtures with alkanes. transferable potentials for phase equilibria. 5. united-atom description of primary, secondary, and tertiary alcohols. *The Journal of Physical Chemistry B*, 105(15):3093, 2001.

[58] S. Pronk, S. Páll, R. Schulz, P. Larsson, P. Bjelkmar, R. Apostolov, M.R. Shirts, J.C. Smith, P.M. Kasson, D. van der Spoel, B. Hess, and E. Lindahl. Gromacs 4.5: a high-throughput and highly parallel open source molecular simulation toolkit. *Bioinformatics*, 29(7):845, 2013.

[59] M.J. Abraham, T. Murtola, R. Schulz, S. Páll, J.C. Smith, B. Hess, and E. Lindahl. Gromacs: High performance molecular simulations through multi-level parallelism from laptops to supercomputers. *SoftwareX*, 1-2:19, 2015.

[60] J.M. Martínez and L. Martínez. Packing optimization for automated generation of complex system's initial configurations for molecular dynamics and docking. *Journal of Computational Chemistry*, 24(7):819, 2003.

[61] R.W. Hockney. *Methods in computational physics, vol. 9*, volume 9, chapter The potential calculation and some applications, pages 135–221. Orlando Academic Press, 1970.

[62] T. Darden, D. York, and L. Pedersen. Particle mesh ewald: An n*log(n) method for ewald sums in large systems. *The Journal of Chemical Physics*, 98(12):10089, 1993.

[63] B. Hess, H. Bekker, H.J.C. Berendsen, and J.G.E.M. Fraaije. Lincs: A linear constraint solver for molecular simulations. *Journal of Computational Chemistry*, 18(12):1463, 1997.

[64] S. Nose. A molecular dynamics method for simulations in the canonical ensemble. *Molecular Physics*, 52(2):255, 1984.

[65] W.G. Hoover. Canonical dynamics: Equilibrium phase-space distributions. *Physical Review A*, 31(3):1695, 1985.

[66] M. Parrinello and A. Rahman. Crystal structure and pair potentials: A molecular-dynamics study. *Physical Review Letters*, 45(14):1196, 1980.

[67] M. Parrinello and A. Rahman. Polymorphic transitions in single crystals: A new molecular dynamics method. *Journal of Applied Physics*, 52(12):7182, 1981.

[68] Imre Bakó, Pál Jedlovszky, and Gábor Pálinkás. Molecular clusters in liquid methanol: a reverse monte carlo study. *Journal of Molecular Liquids*, 87(2):243–254, 2000. Associated Fluids and Ionic Systems Vth Liblice Conference on Statistical Mechanics of Liquids.

[69] Ralf Ludwig. The structure of liquid methanol. *ChemPhysChem*, 6(7):1369–1375, 2005.

[70] A. Vrhovšek, O. Gereben, A. Jamnik, and L. Pusztai. Hydrogen bonding and molecular aggregates in liquid methanol, ethanol, and 1-propanol. *The Journal of Physical Chemistry B*, 115(46):13473–13488, 2011. PMID: 21916497.

[71] M. Požar, B. Lovrinčević, L. Zoranić, T. Primorac, F. Sokolić, and A. Perera. Micro-heterogeneity versus clustering in binary mixtures of ethanol with water or alkanes. *Physical Chemistry Chemical Physics*, 18:23971–23979, 2016.

[72] Henry S. Frank and Wen-Yang Wen. Ion-solvent interaction. structural aspects of ion-solvent interaction in aqueous solutions: a suggested picture of water structure. *Discuss. Faraday Soc.*, 24:133–140, 1957.

[73] J.W. Perram and S. Levine. Cooperative hydrogen bonding and the question of flickering clusters in water. *null*, 21(4):701–708, January 1971.

[74] S. Sarkar and R. N. Joarder. Molecular clusters and correlations in liquid methanol at room temperature. *The Journal of Chemical Physics*, 99:2032–2039, 1993.

[75] S. Sarkar and R. N. Joarder. Molecular clusters in liquid ethanol at room temperature. *The Journal of Chemical Physics*, 100:5118–5122, 1994.

[76] B. Kežić, R. Mazighi, and A. Perera. A model for molecular emulsions: Water and âweak waterâ mixtures. *Physica A: Statistical Mechanics and its Applications*, 392(4):567–582, 2013.

[77] J.-H. Guo, Y. Luo, A. Augustsson, S. Kashtanov, J.-E. Rubensson, D. K. Shuh, H. Ågren, and J. Nordgren. Molecular structure of alcohol-water mixtures. *Phys. Rev. Lett.*, 91:157401, Oct 2003.